Dynamical scaling analysis of phase transition and critical properties for the RP^2 model in two dimensions

Yukiyasu Ozeki, Atsuyuki Matsuda, and Yuki Echinaka
Department of Engineering Science, Graduate School of Informatics and Engineering, The University of Electro-Communications, 1-5-1 Chofugaoka, Chofu-shi, Tokyo 182-8585, Japan

(Received 21 June 2018; revised manuscript received 3 October 2018; published 11 January 2019)

The phase transition and critical properties for the RP^2 model in two dimensions is investigated by means of the nonequilibrium relaxation method (NER) together with the dynamical scaling analysis. The relaxation of nematic order from the all-aligned state is observed by Monte Carlo simulations. The comparison of types of the asymptotic form of the relaxation time around the transition point is considered by the dynamical scaling analysis, which clearly discriminates the Kosterlitz-Thouless (KT)-type transition from the second-order one. Using the relaxation of fluctuation, the static critical exponent η and the dynamical one z, which are only the intrinsic exponents for the KT transition, are estimated at and below the KT transition temperature. The result shows similar behaviors with those observed in the KT phase for the ferromagnetic XY model in two dimensions, which has been recognized as a typical KT system, and reveals the confirmation of the present KT transition.

DOI: 10.1103/PhysRevE.99.012116

I. INTRODUCTION

In two dimensions, since Mermin and Wagner's remarkable study [1], it has been well-known that the continuous spin systems with short-range interactions show no long-range order. Then, a quasi-long-range order without spontaneous symmetry breaking was proposed for the XY model, which is called the Kosterlitz-Thouless (KT) transition [2,3]. In this phase, there is no spontaneous magnetization, but the correlation length always diverges, and now the transition is recognized by the scenario of the binding-unbinding behavior of vortex pairs. As for the Heisenberg cases, of course, there exists no long-range order, and further the KT transition is also denied for the bilinear interactions.

However, there have been various discussions on the phase transition for the RP^2 model in two dimensions, which consists of Heisenberg spins with nearest-neighboring biquadratic interactions. In three dimensions, it has been considered that the RP^2 model shows a weak first-order transition, while that in two dimensions shows KT transition with a quasi-long-range order [4–7]. In this case, the topological point defects caused by the Z_2 vortices are stable instead of the integer-vortices in the standard KT phase in the XY model. However, some studies show the possibility that a phase transition doesn't exist at finite temperature [8,9].

In the present study, we investigate the phase transition and critical properties for the RP^2 in two dimensions by means of the nonequilibrium relaxation (NER) method [10]. Using Bayesian statistics and the kernel method, we have developed an improved dynamical scaling analysis scheme for KT transition in the NER method [11]. This analysis allows data to be fitted efficiently to a scaling function without using any parametric model function. It makes the results more precise and reliable, and can be applied to the method for the confirmation of the transition type. Comparing the assumptions for the asymptotic form of the relaxation time, we confirm the transition type as the KT one. As a successful example, we apply this dynamical scaling analysis of NER data to confirm the existence of the KT transition for the present model. We also estimate the critical exponents by means of the relaxation of fluctuation [12,13], where the static exponent η and the dynamical one$z$ can be defined for the KT case. In the regime below the transition temperature, since it is always critical inside the KT phase, these exponents are estimated there, and we examine the temperature dependence of η and z compared with KT phase for other models.

The remainder of this paper is organized as follows. The RP^2 model is introduced, and a typical relaxation of order parameter is calculated in Sec. II. The NER method and its improved dynamical scaling analysis are explained in Sec. III. In Sec. IV, the comparison of KT transition and its confirmation are discussed. Critical exponents are estimated at and below the KT transition temperature in Sec. V. Section VI gives some remarks.

II. RP^2 MODEL

We examine the RP^2 model in two dimensions, in which classical Heisenberg spins show the global $O(3)$ symmetry. Unlike to the standard Heisenberg ferromagnet, the Hamiltonian contains the square of the inner product between neighboring spins representing a nonpolar spin system and is expressed by

$$\mathcal{H} = -J \sum_{\langle ij \rangle} (\mathbf{S}_i \cdot \mathbf{S}_j)^2 = -J \sum_{\langle ij \rangle} \cos^2 \Delta\theta_{ij}, \qquad (1)$$

where the summation is taken over all nearest-neighboring sites on the square lattice, $\mathbf{S}_i$ is a classical Heisenberg spin and $\Delta\theta_{ij}$ is the angle between two spins. The model is also known as the Lebwohl-Lasher model [14] for the nematic transition in liquid crystals. This system has been studied by another Hamiltonian with a shifted origin and a different energy

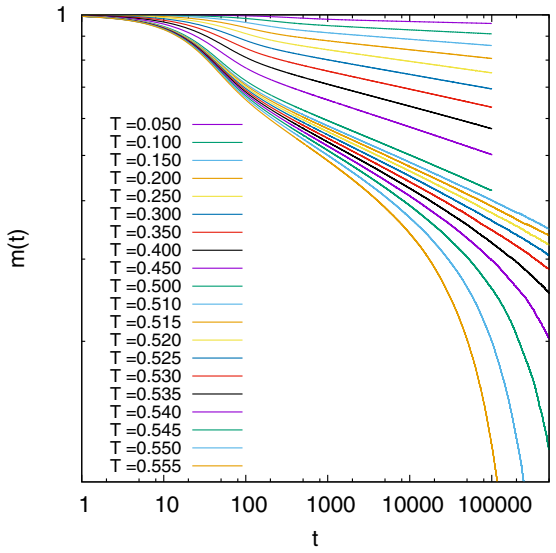

FIG. 1. Relaxation of order parameter $m(t)$ plotted on a double logarithmic scale calculated on 1501×1500 lattice for $T \leqslant 0.500$ and on 901×900 lattice for $T \geqslant 0.510$.

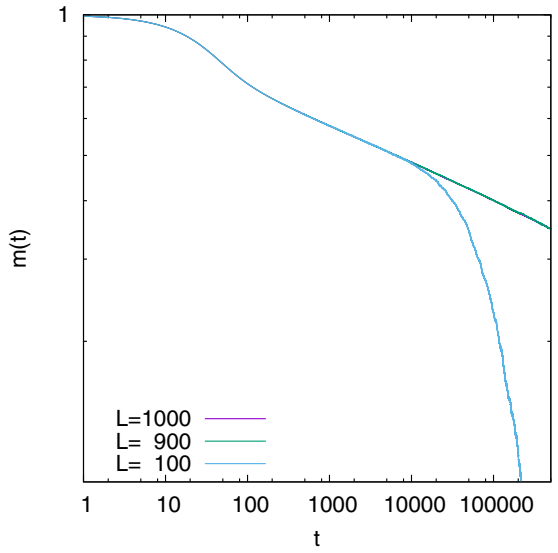

FIG. 2. Size dependence of the relaxation at $T = 0.51$. For the case of $L = 100$, the curve is deviated from those of the larger sizes around $t = 10^4$ showing the finite-size effect. For the case of $L = 900$, the curve coincides with that of $L = 1000$ up to $t = 2 \times 10^5$ confirming no size dependence.

scale as

$$\mathcal{H} = -J \sum_{\langle ij \rangle} P_2 (\mathbf{S}_i \cdot \mathbf{S}_j) = -J \sum_{\langle ij \rangle} \frac{1}{2}(3\cos^2 \Delta\theta_{ij} - 1), \quad (2)$$

where P_2 is the Legendre polynomial of the second degree:

$$P_n(x) = \frac{1}{2^n n!} \frac{d^n}{dx^n}[(x^2 - 1)^n]. \quad (3)$$

Since the physical properties are the same between these two models, we use the Hamiltonian as Eq. (2) in the following analysis.

In the NER analysis, we simulate a relaxation process from the all-aligned state along the z-direction, and observe the order parameter for the nematic ordering,

$$m = \frac{1}{N} \sum_i P_2 (\cos \theta_i) = \frac{1}{N} \sum_i \frac{1}{2}(3\cos^2 \theta_i - 1), \quad (4)$$

where θ_i is the angle to the z direction, representing $S_{iz} = \cos \theta_i$. Asymptotically in a long time, this order parameter remains a spontaneous value in the nematic phase in higher dimensions. In the KT phase, if it exists, it shows a power-law decay in the asymptotic region.

To analyze the transition, we perform Monte Carlo simulations for the RP^2 model in two dimensions and observe the relaxation of the order parameter $m(t) \equiv \langle m \rangle_t$. Calculations were carried out on 901×900 and 1501×1500 square lattices with skew boundary conditions up to an observation time of 2×10^5 Monte Carlo steps (MCSs). We use the skew boundary condition for the purpose of efficient calculations. About 1024 independent samples were taken for statistical averaging at each temperature. Hereafter, we measure the temperature in the unit of J/k_B. The result is shown in Fig. 1. In the standard NER analysis, one needs relaxation properties in the thermodynamic limit to avoid the finite size effect in dynamical scaling analysis. It can be achieved by checking the size dependence in the interval of observed MCSs. In a Monte Carlo simulation, the correlation length $\xi(t)$ evolves monotonically from zero (at $t = 0$) to a large value around the critical temperature. The finite size effect appears when $\xi(t)$ reaches to the system size. We confirm that the size used in the present simulation, 901×900, is large enough to avoid the finite size effect in the interval less than 2×10^5 MCSs. As an example, we show a comparison of relaxation data in Fig. 2 for 101×100, 901×900 and 1001×1000 at $T = 0.51$ where the expected transition temperature is close to.

III. DYNAMICAL SCALING FOR NONEQUILIBRIUM RELAXATION

The NER analysis for an equilibrium phase transition is based on the relaxation of the order parameter $m(t, T)$, by which one can estimate the transition temperature, and a dynamical exponent. It is expected that $m(t, T)$ decays to zero exponentially in the paramagnetic (PM) phase, and the algebraic decay appears at and below the KT transition temperature. The asymptotic behavior of the order parameter is expected to be

$$m(t, T) \sim \begin{cases} \exp(-t/\tau) & (T > T_{\mathrm{KT}}) \\ t^{-\lambda(T)} & (T \leqslant T_{\mathrm{KT}}) \end{cases}. \quad (5)$$

The dynamical exponent $\lambda(T)$, the asymptotic power of the relaxation, is defined whole in the KT phase and depends on the temperature. Let us see the relaxation behavior plotted in Fig. 1 in a double-logarithmic scale. For $T > 0.51$, one can see the downward trend in the asymptotic regime, which indicates the exponential decay in the PM phase. However, for $T < 0.51$, the asymptotic behaviors seems straight up to the observed MCSs, which is consistent with the relaxation in the KT phase. Note that, unlike to the second-order transition case, one cannot estimate the lower bound of T_{KT}, but the upper bound in the KT case.

To confirm the KT transition and estimate the transition temperature, we have introduced a dynamical scaling analysis based on the following natural scaling form [15]:

$$m(t, T) = \tau^{-\lambda}\Psi(t/\tau). \tag{6}$$

The relaxation time τ depends on the temperature, and is expected to diverge at the KT transition temperature with the asymptotic form

$$\tau(T) = a \exp\left(\frac{b}{\sqrt{T - T_{\rm KT}}}\right), \tag{7}$$

similarly as the correlation length does. Note that the same dynamical scaling Eq. (6) can also be applied to the second-order transition, where a typical power-law form

$$\tau(T) = a|T - T_c|^{-b} \tag{8}$$

is substituted for the asymptotic form of the relaxation time.

Here, we interpret the dynamical scaling analysis improved previously [11], and follow the formalism what is shown there for the self-containedness. To estimate $T_{\rm KT}$, we can use $m(t, T)$ in a sufficient interval of MC steps for several values of T, and fit the data to the above formula. Let us use the label i for all data points as $m(t_i, T_i)$. The corresponding relaxation time is also dependent on i, i.e., τ_i, which should be identical for those with the same temperature, i.e., $\tau_i = \tau_j$ when $T_i = T_j$. If one assumes the scaling law, all data points converted as

$$X_i \equiv t_i/\tau_i, \tag{9a}$$

$$Y_i \equiv \tau_i^{\lambda} m(t_i, T_i), \tag{9b}$$

$$E_i \equiv \tau_i^{\lambda} \delta m(t_i, T_i) \tag{9c}$$

should collapse according to a scaling function as

$$Y_i = \Psi(X_i), \tag{10}$$

where $\delta m(t_i, T_i)$ is the statistical error of $m(t_i, T_i)$ estimated in the simulation, and E_i is that of Y_i. Estimating the critical exponent and corresponding transition temperature is known as dynamical scaling analysis.

To perform the scaling fit efficiently, we use the dynamical scaling analysis proposed previously [11]. Assuming the posterior probability as a multivariate Gaussian distribution, the log-likelihood function can be written as

$$\log L(\vec{\theta}_p, \vec{\theta}_h) \equiv -\frac{1}{2}\log|2\pi\Sigma| - \frac{1}{2}(\vec{Y} - \vec{\Psi})^t \Sigma^{-1}(\vec{Y} - \vec{\Psi}), \tag{11}$$

where Σ is the covariance matrix and

$$(\vec{Y})_i \equiv Y_i, \tag{12}$$

$$(\vec{\Psi})_i \equiv \Psi(X_i). \tag{13}$$

Using the kernel method, we assume that the covariance matrix is expressed by the kernel function, and the Gauss kernel function is used in the Bayesian inference with a Gauss process regression [11,16]. Then, the covariance matrix Σ in Eq. (11) is obtained by

$$(\Sigma)_{ij} = \begin{cases} \theta_1^2 \exp\left(-\frac{(X_i - X_j)^2}{2\theta_2^2}\right) & (i \neq j) \\ \theta_0^2 + \theta_1^2 + E_i^2 & (i = j) \end{cases}, \tag{14}$$

where θ_0, θ_1, and θ_2 are hyper parameters for the Gauss kernel function. In this study, we perform dynamical scaling for the logarithms of X_i and Y_i as

$$X_i' \equiv \log X_i = \log t_i - \left(\log a + \frac{b}{\sqrt{T_i - T_{\rm KT}}}\right),$$

$$Y_i' \equiv \log Y_i = \log m(t_i, T_i) + \lambda\left(\log a + \frac{b}{\sqrt{T_i - T_{\rm KT}}}\right),$$

$$E_i' \equiv \log\left(1 + \frac{E_i}{Y_i}\right) \approx \frac{E_i}{Y_i} = \frac{\delta m(t_i, T_i)}{m(t_i, T_i)}. \tag{15}$$

We used ten values of temperatures above the transition temperature, where the downward trend is observed in Fig. 1, and sampled 100 points for each temperature as shown in Fig. 3, so as to give equal intervals of $\log t$ (the X axis). To maximize the log-likelihood function Eq. (11), the parameters, $T_{\rm KT}$, λ, a, b, θ_0, θ_1, and θ_2 appearing in Eqs. (6), (7), and (14) are optimized. We use the conjugate gradient algorithm [17] to maximize the log-likelihood function practically, where the iterations are performed by modifying the parameters along the direction of steepest descent. The results are shown in Fig. 4 with $T_{\rm KT} = 0.50764$ and $\lambda = 0.069$. It is noted that we do not consider so-called the logarithmic correction, which has been pointed out for the analysis of static correlation, since there is an argument for negligible of it in the dynamical case [18]. In our dynamical analysis, we simulate on sufficiently large lattices so that the size dependence does not appear up to the maximum observed MCS, which can be recognized almost an infinite lattice. Thus, if the logarithmic correction observed in scaling analysis for finite systems appears because of the finiteness, our dynamical data could be free to that. This conjecture is consistent with our previous results, however we can not show the validity of it at

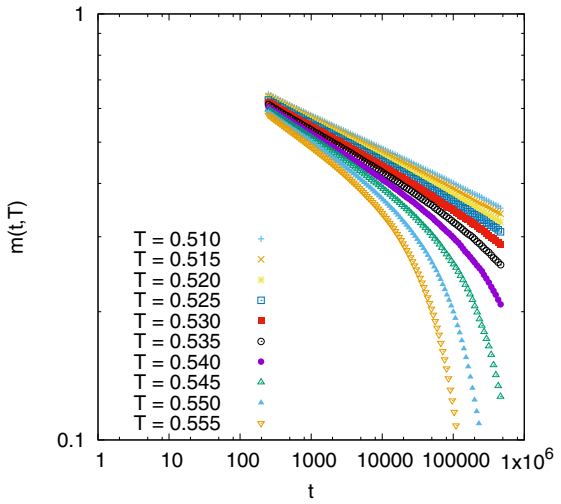

FIG. 3. Relaxation of order parameter for selected temperatures plotted on a double-logarithmic scale. For each temperature, 100 data points are chosen so as to give equal intervals on the horizontal axis.

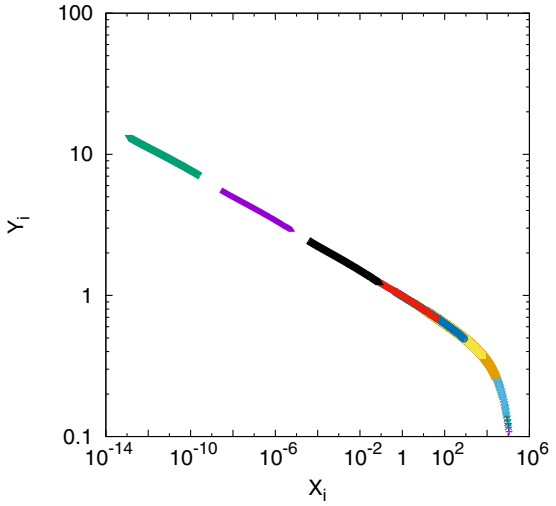

FIG. 4. Scaling plot for the date in Fig. 3 with $T_{\rm KT} = 0.50764$ and $\lambda = 0.069$.

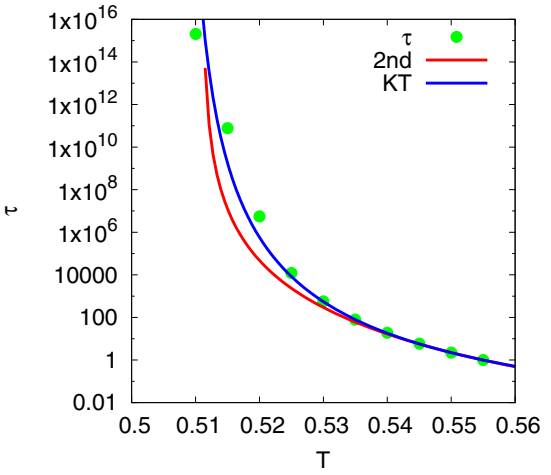

FIG. 5. Estimated relaxation time τ. Three different dynamical scaling results are plotted for the function $\tau(T)$ under the assumption of a second-order transition, KT transition, and without assumption (closed circles).

present. To confirm it, we need a model for a benchmark test in which the exact transition temperature is known. It remains a future problem.

IV. CONFIRMATION OF KT TRANSITION

To support the confirmation of the KT transition, we apply the method for the discrimination of transition type by the use of the NER data. In the previous paper, we proposed a numerical scheme to confirm the KT transition by the use of the following dynamical scaling [11]. Let us fit the relaxation data by introducing the values of τ for all temperatures as the fitting parameters, rather than using the asymptotic form of τ. If, for example, the temperatures of the simulated data are $T_1, T_2, \cdots, T_M$, the corresponding τ values, i.e., $\tau_1, \tau_2, \ldots, \tau_M$, are introduced and optimized by a similar scaling process. This provides the temperature dependence of τ for the chosen temperatures without any assumption regarding its asymptotic form. Together with the dynamical scaling for the assumption of the algebraic divergence of $\tau(T)$, Eq. (8), we have three different dynamical scaling results for the function $\tau(T)$: (i) assumption of second-order type using Eq. (8), (ii) assumption of KT type using Eq. (7), and (iii) no assumption of the transition type. We can compare them to determine the most suitable transition type.

Note that, even if the assumption of one particular transition type is correct and the assumed asymptotic function is suitable, the result cannot give a better fit than that without any assumption. Thus, one can discriminate the transition type by checking how close the result with some assumption is to that without the assumption. Such a comparison could take many forms; we have proposed the following residual for the logarithm of τ, defined by

$$r = \frac{1}{M}\sum_{m=1}^{M}\{\log\tau(T_m) - \log\tau_m\}^2, \tag{16}$$

where $\tau(T_m)$ is estimated through the assumption (i) or (ii) using Eqs. (8) or (7), respectively, and τ_m is estimated through no assumption, i.e., (iii). While this function would not be the best choice for the analysis, it has worked very well for some benchmark cases [11].

We perform three types of dynamical scaling for the relaxation data in Fig. 3. For type (i), we obtain the transition temperature as $T_{\rm c} = 0.51111$. The result in the previous section is used for the type (ii). Together with the result for type (iii), the τ values are plotted in Fig. 5. At a glance, the curves of τ for assumption (ii) is more suitable than that for assumption (i), indicating the KT transition. For a more precise comparison, we used the residual defined in Eq. (16). This gives $r_{\rm 2nd} = 11.3$ for the assumption of the second-order transition and $r_{\rm KT} = 2.17$ for the assumption of the KT transition. The residual for the assumption of the KT transition is suitable and several times smaller than that for the second-order type. This result for the confirmation of the KT transition is also supported by the following observation. As seen in Fig. 5, the curve for the second-order transition shows diverging at temperatures greater than $T = 0.51$, which is inconsistent with the estimation of the finite value of $\tau(T)$ at $T = 0.51$, indicating the PM phase. This reveals the identification of the correct KT transition.

Since it has been clearly known that the second-order transition cannot appear in the present model because of the Mermin and Wagner's theorem [1], the above result for the preference of the KT transition can be recognized as an evidence for the existence of that transition. Therefore, while seeking the best choice for the cost function instead of the residual Eq. (16) is important for the present dynamical method, we would not do it in this paper. It remains a future problem.

V. EVALUATION OF CRITICAL EXPONENTS DUE TO RELAXATION OF FLUCTUATION

Let us consider the critical exponents. For the KT transition point, the intrinsic critical exponents are only the static one η and the dynamical one z. In the case inside the KT phase, the thermodynamics keeps critical, and the correlation length

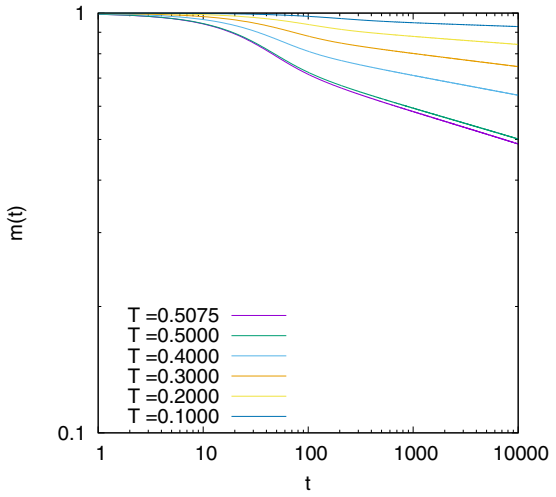

FIG. 6. Relaxation of order parameter $m(t)$ at and below the estimated transition temperature $T_{\rm KT} = 0.5075$.

always diverges. Therefore, one can define the exponents η and z whole inside the KT phase. We estimate these exponents and compare the temperature-dependence with those for the ferromagnetic (FM) XY model in two dimensions, which has previously been investigated well.

We have proposed the NER analysis of critical exponents for KT transition systems applying the NER of fluctuation like in the case of second-order transitions [10]. At the transition point, we assume a power-law relaxation of order parameter

$$m(t) \sim t^{-\lambda}. \tag{17}$$

Previously, we showed the relation [13]

$$\lambda = \frac{\eta}{2z}. \tag{18}$$

To estimate the exponents η and z separately, we use a relaxation of fluctuation,

$$f_{mm}(t) \equiv N\left\{\frac{m_2(t)}{m(t)^2} - 1\right\}, \tag{19}$$

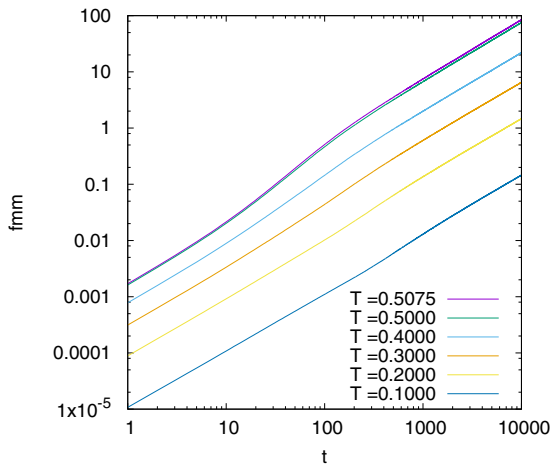

FIG. 7. Relaxation of fluctuation $f_{mm}(t)$ at and below the estimated transition temperature.

where

$$m_2(t) \equiv \left\langle \left(\frac{1}{N} \sum_i P_2(\cos\theta_i) \right)^2 \right\rangle_t. \tag{20}$$

This function diverges algebraically at the KT transition point,

$$f_{mm}(t) \sim t^{\lambda_{mm}}, \tag{21}$$

as $t \to \infty$ with the exponent

$$\lambda_{mm} = \frac{2}{z}. \tag{22}$$

It is convenient to define the local exponents for $m(t)$ and $f_{mm}(t)$ as

$$\lambda(t) \equiv -\frac{d\log m(t)}{d\log t}, \tag{23}$$

$$\lambda_{mm}(t) \equiv \frac{d\log f_{mm}(t)}{d\log t}. \tag{24}$$

Using Eqs. (18) and (22) together with Eqs. (23) and (24), we obtain the following local exponents:

$$z(t) \equiv \frac{2}{\lambda_{mm}(t)}, \tag{25}$$

$$\eta(t) \equiv \frac{4\lambda(t)}{\lambda_{mm}(t)}, \tag{26}$$

which approach to conventional exponents z and η respectively with $t \to \infty$. The above argument can be used also to estimate the exponents inside the KT phase, and Eqs. (18), (22), (25), and (26) can be applied.

We calculate $m(t)$ and $f_{mm}(t)$ for the estimated transition temperature $T_{\rm KT} = 0.5075$ together with several ones ($T = 0.1, 0.2, 0.3, 0.4, 0.5$) below $T_{\rm KT}$. Calculations were carried out on a 401×400 square lattice with skew boundary conditions up to an observation time of 10^4 MCSs. About 4×10^5 independent samples were taken for statistical averaging at each temperature. The results are shown in Figs. 6 and 7. From these figures, we obtain numerical evaluations of the

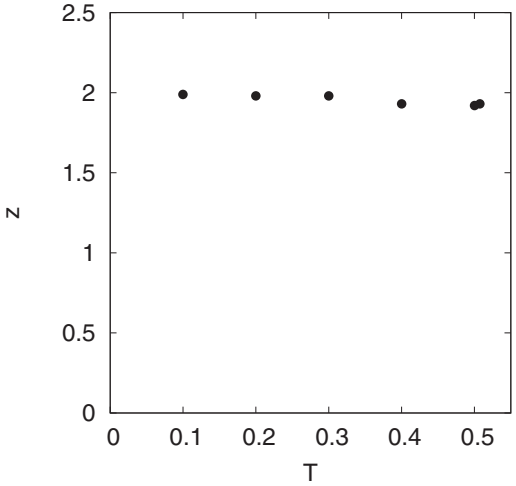

FIG. 8. Estimated dynamical exponent z at and below the transition temperature. The constantness around $z \sim 2$ is observed whole in the KT phase.

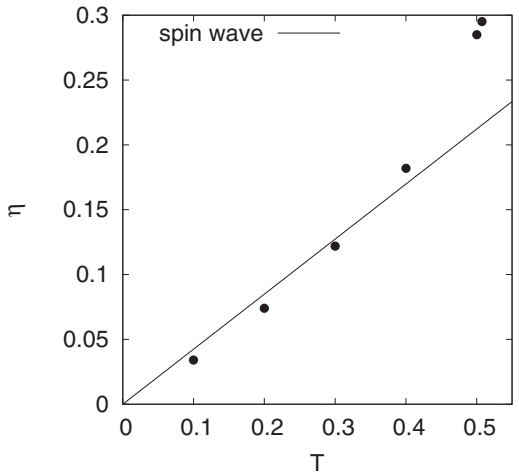

FIG. 9. Estimated static exponent η at and below the transition temperature. The solid line indicates the result by the spin wave theory in the KT phase.

logarithmic derivatives, Eqs. (23) and (24), for each temperature. Then, we estimate the asymptotic values of Eqs. (25) and (26) and obtain the exponents shown in Figs. 8 and 9. Note that corrections to scaling are considered in the estimation of exponents automatically (while not completely), since, in the extrapolation for $1/t \to 0$, intermediate values with $1/t > 0$ deviate from the asymptotic one with $1/t = 0$ and the estimates are treated to converge to such deviations.

It is observed in Fig. 8 that the dynamical exponent z behaves almost $z = 2$ whole in the low temperature phase. This behavior in low-temperature regime for the RP^2 model is quite similar with that for the FM XY model in two dimensions [2,13]. It is also observed in Fig. 9 that the temperature dependence of the static exponent $\eta(T)$ is consistent with the result of the spin wave theory,

$$\eta = \frac{4T}{3\pi}, \tag{27}$$

around $T \sim 0$. The consistency with the spin wave theory have also been seen in the FM XY model [13]. A similar observation has been reported by means of the equilibrium simulations [9], where the authors claimed the small discrepancy among the estimations of η and concluded the absence of the KT transition. While the numerical result for η is quite similar, we would like to argue that the validity for the KT transition has been supported in the previous section as well as the present result for the temperature dependence of z and η. Consequently, these observations support the confirmation of the KT transition and the KT phase in the present model.

VI. REMARKS

We investigate the phase transition and critical properties for the RP^2 model in two dimensions. The nonequilibrium relaxation method (NER) is used together with the dynamical scaling analysis developed recently. As an order parameter, the relaxation of nematic order from the all-aligned state is observed by the Monte Carlo simulation with the standard Metropolis algorithm. In the dynamical scaling analysis for the order parameter, the comparison of the type of the asymptotic form of the relaxation time around the transition point clearly discriminates the Kosterlitz-Thouless (KT) type transition from the second-order one. Furthermore, using the relaxation of fluctuation, we estimate the static critical exponent η and the dynamical one z, which are only the intrinsic exponents for the KT transition, at the transition point as well as inside the KT phase. The result shows similar behaviors with those observed in the KT phase for the FM XY model in two dimensions, which has been recognized as an typical KT system, and reveals the confirmation of the present KT transition. Especially, we emphasize that it would be the first time in the society to observe the temperature-independent dynamical exponent $z \sim 2$ for the present model, which has been reported for the FM XY model.

ACKNOWLEDGMENTS

This work was supported by JSPS KAKENHI Grant No. 15K05205. The authors thank Y. Tomita for fruitful discussions and comments. The authors are also grateful to the Supercomputer Center at the Institute for Solid State Physics, University of Tokyo, for the use of their facilities.

[1] N. D. Mermin and H. Wagner, Phys. Rev. Lett. **17**, 1133 (1966).
[2] V. L. Berezinskii, Sov. Phys. -JETP **32**, 493 (1971).
[3] J. M. Kosterlitz and D. J. Thouless, J. Phys. C: Solid State **6**, 1181 (1973).
[4] C. Chiccoli, P. Pasini, and C. Zannoni, Physica. A **148**, 298 (1988).
[5] H. Kunz and G. Zumbach, Phys. Rev. B **46**, 662 (1992).
[6] E. Mondal and S. K. Roy, Phys. Lett. A **312**, 397 (2003).
[7] S. Dutta and S. K. Roy, Phys. Rev. E **70**, 066125 (2004).
[8] R. Paredes V., A. I. Fariñas-Sánchez, and R. Botet, Phys. Rev. E **78**, 051706 (2008).
[9] A. I. Farinas-Sànchez, R. Botet, B. Berche, and R. Paredes, Cond. Matter Phys. **13**, 13601 (2010).
[10] Y. Ozeki and N. Ito, J. Phys. A: Math. Theor. **40**, R149 (2007).
[11] Y. Echinaka and Y. Ozeki, Phys. Rev. E **94**, 043312 (2016).
[12] N. Ito, K. Ogawa, K. Hukushima, and Y. Ozeki, Prog. Theor. Phys. Suppl. **138**, 555 (2000).
[13] Y. Ozeki, S. Yotsuyanagi, T. Sakai, and Y. Echinaka, Phys. Rev. E **89**, 022122 (2014).
[14] P. A. Lebwohl and G. Lasher, Phys. Rev. A **6**, 426 (1972).
[15] Y. Ozeki, K. Ogawa, and N. Ito, Phys. Rev. E **67**, 026702 (2003).
[16] K. Harada, Phys. Rev. E **84**, 056704 (2011).
[17] E. Polak, *Computational Methods in Optimization* (Academic Press, New York, 1971).
[18] H. P. Ying, B. Zheng, Y. Yu, and S. Trimper, Phys. Rev. E **63**, 035101(R) (2001).